



# Grain growth in the envelopes of Class I protostars

A. Miotello<sup>1,2,3,4</sup>, L. Testi<sup>1,5,6</sup>, G. Lodato<sup>2</sup>, L. Ricci<sup>7</sup>, G. Rosotti<sup>3,5</sup>, K. Brooks<sup>8</sup>, A. Maury<sup>9</sup>, A. Natta<sup>6,10</sup>

<sup>1</sup> European Southern Observatory, <sup>2</sup> University of Milan, <sup>3</sup> MPE Garching, <sup>4</sup> Leiden Observatory, <sup>5</sup> Excellence Cluster Universe, <sup>6</sup> INAF-Arcetri, <sup>7</sup> CALTECH, <sup>8</sup> ATNF, <sup>9</sup> CFA, <sup>10</sup> DIAS

?

Many observational results (Testi et al. PPVI review) indicate that the vast majority of the protoplanetary disks in the Class II phase contain mm- and cm-sized grains. This implies that the formation of these large particles is a fast process that occurs in the early stages of disks or possibly even earlier. Pagani et al. (2011) have shown that micron-sized grains are already present in prestellar cores, while mm-sized particles may have been detected in Class 0 YSOs envelopes (Chiang et al. 2012).

## GOAL

The aim of this work is to constrain the level of grain growth in Class I YSOs, where the contribution of the envelope emission can be separated by the disk one, using mm-interferometry.

## RESULTS

- mm-sized pebbles in the envelopes
- Very compact embedded disks

## Analysis

- Fig. 1 and 3: visibility amplitudes of Elias29 and WL12: with archival 1.1 mm SMA data (Jørgensen et al. 2009) and new 3 mm ATCA dataset.
- Emission rises at the shortest baselines: presence of an envelope
- Emission at the long baselines converge to a constant non-zero value: presence of an unresolved embedded disk.
- Under the optically thin assumption and the Rayleigh-Jeans approximation: unusually low  $\alpha$ , for both disk and envelope.
- Modeling of the disk and envelope structures, using radiative transfer codes, is needed.

## Disk modeling

- Two-layer disk model (Dullemond et al. 2001). Free parameters: disk outer radius  $R_{out}$ , mass  $M_{disk}$  and the grains maximum size  $a_{max}$ .

## Envelope modeling

- Rotating and collapsing envelope model as derived by Ulrich et al. 1976.
- Envelope temperature structure computed using the Monte Carlo radiative transfer code RADMC-3D (Dullemond & Dominik 2004). Central heating source star+disk.
- Envelope mass  $M_{env}$  and  $a_{max}$  left free to vary.

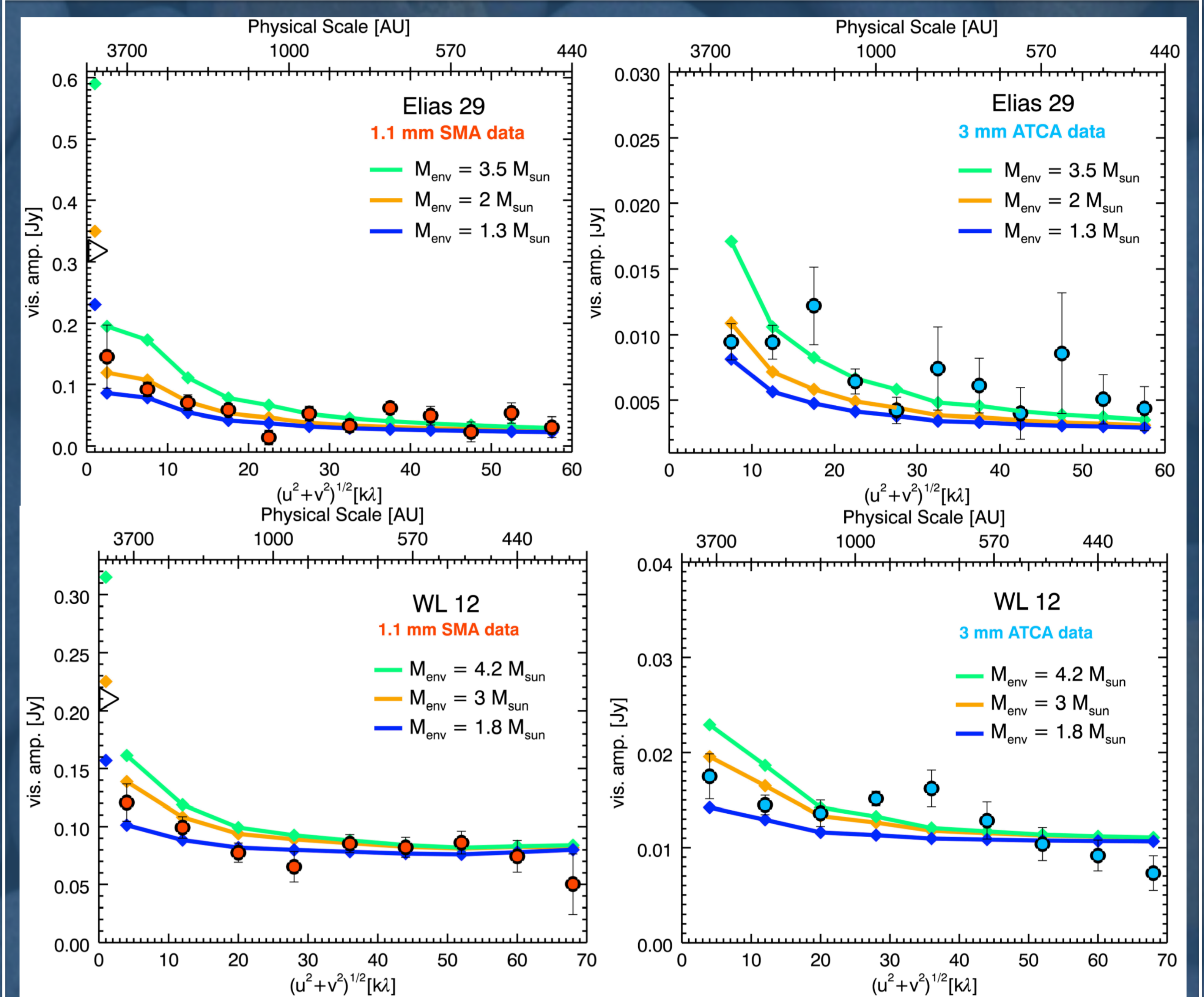
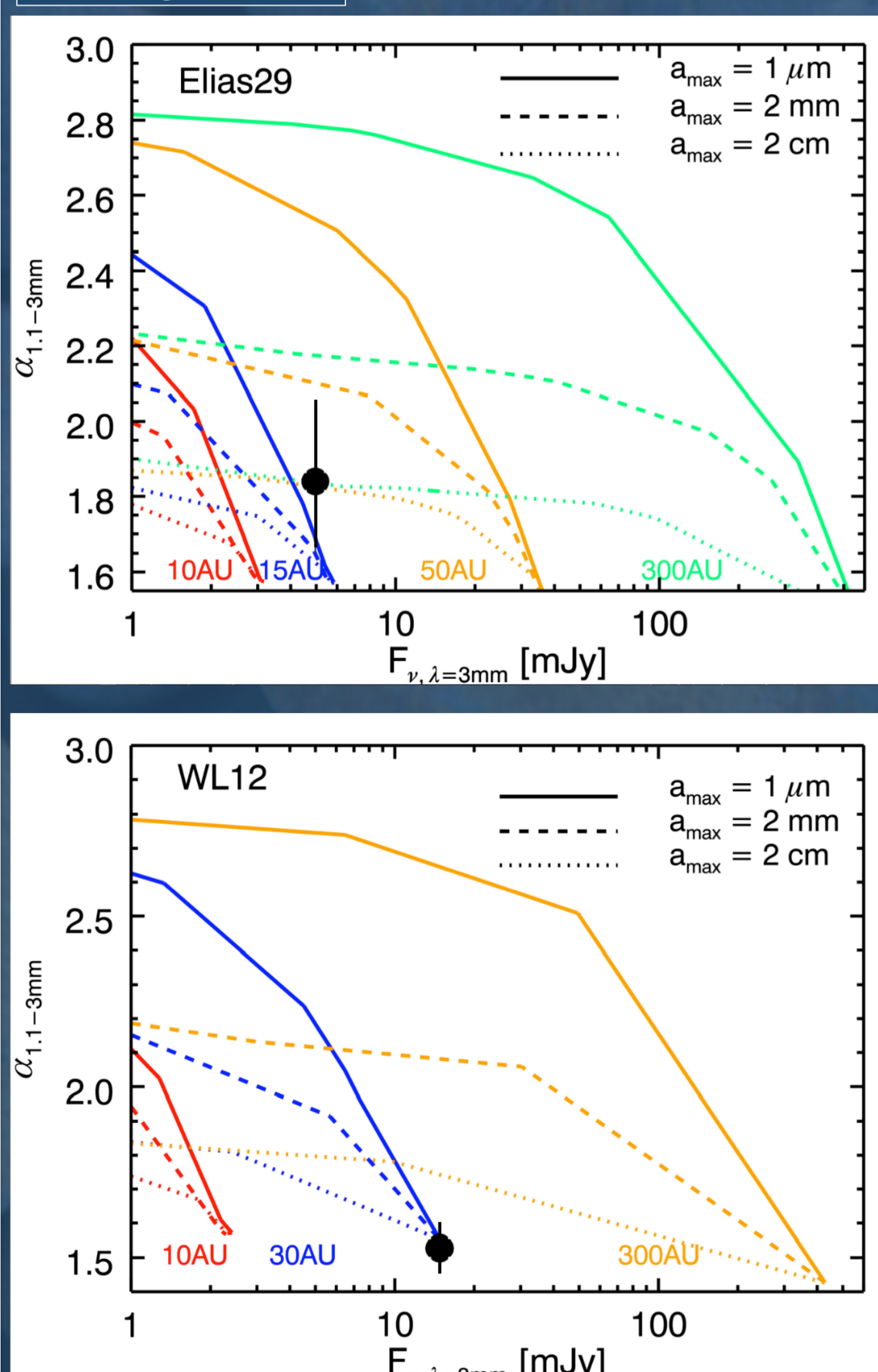


Fig. 1

Visibility amplitudes. The data points give the amplitudes per bin. Amplitudes of Elias 29 (top panels) and WL12 (bottom panels): on the left, archival 1.1 mm SMA dataset (Jørgensen et al. 2009), on the right new 3 mm ATCA dataset. The open triangles: zero spacing 1.1 mm fluxes, interpolated between 850  $\mu\text{m}$  and 1.25 mm single dish fluxes (Lommen et al. 2008; Jørgensen et al. 2009). Orange lines are the best fits, obtained using the two-layer disk model (Dullemond et al. 2001) combined with a rotating and collapsing envelope model implemented on RADMC-3D (Dullemond & Dominik 2004).

Fig. 2



## Compact disks

- Elias 29
  - Either a small optically thick disk ( $R_{out} \sim 15$  AU,  $M_{disk} \sim 0.07 M_{sun}$ ), where we cannot constraint the dust properties, or a relatively large ( $R_{out} \sim 50-200$  AU) optically thin disk populated with large pebbles.
- WL12
  - Compact and optically thick disk with radius  $R_{out} \sim 30$  AU and mass between 0.3 and 0.8 solar masses. We can not constrain the dust properties.

## Big grains in the envelopes

- Micrometer-sized grains do not explain the observations both at 1mm and 3 mm, while mm-sized ones do (Fig.3).

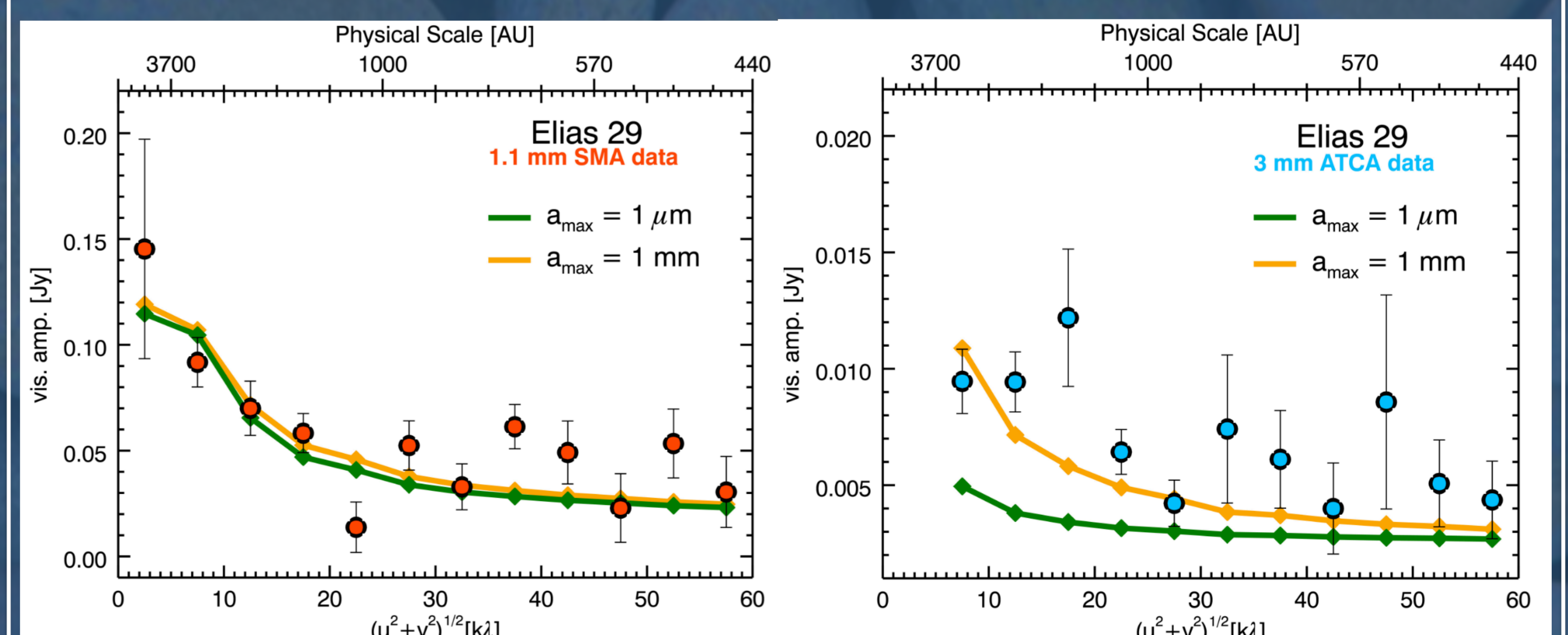


Fig. 3